Author Response to the Public Discussion of "*Technical Note: Disentangling the groundwater response to Earth and atmospheric tides to improve subsurface characterisation*" by Gabriel C. Rau *et al.*

First off, we thank the Editor and reviewers for their efforts in handling, reading, assessing, and reviewing our discussion article published in HESSD. We have received positive and constructive comments during the public discussion and review. We now take the opportunity to reply to all these comments in more detail. We note that none of the comments have provided criticism that could alter the overall message. We hope that our replies will lead to the decision that we can revise the manuscript and, finally, to a consideration for publication in HESS. To make the assessment easier, we have colour coded our replies in the categories agreed (green), partially agreed (orange) and disagreed (red). Our explanations of changes to the manuscript are highlighted in blue colour.

Additional revisions that go beyond the reviewers' recommendations:

- We have double checked all equations and found a few errors that were corrected.
- We renamed the harmonic estimation of amplitudes and phases (previously named APES) to HALS (standing for HArmonic Least-Squares).
- We made a small enhancement of Figure 4.

Please refer to the tracked changes manuscript which highlights all the changes made. Line numbers refer to the revised document without track changes marked.

Referee Comments 1 (Tod Rasmussen):

As one of the cited authors (Rasmussen), I was especially interested in the application of this methodology and the resultant conclusions. The authors' application of deconvolution in the time domain, and its comparison to frequency domain results are novel and something that I have been eagerly awaiting. The consistency between results is striking, leading to increased confidence in system characterization. To summarize the novelty; I (and others) have examined the response of water levels to exogenous influences (e.g., barometric pressure, precipitation, Earth tides, evapotranspiration) using time-series regression deconvolution. The resulting response functions are then used to estimate aquifer, aquitard, and vadose zone properties. Alternatively, many others have developed relationships between water levels and exogenous variables in the frequency domain for periodic and aperiodic influences. What has been missing, until now, is a comparison of these two methods. It is especially gratifying to note the similar results between the two fundamentally different methods, leading to reduced parameter uncertainties and improved robustness. It would be interesting to apply this methodology to other situations, which the tools that the authors provide have made possible.

We thank Todd for his valuable time and positive feedback. While these comments do not necessitate any revisions, we realise that it would be good to include a message that our comparison is valuable for the community.

We did not see the need to revise our manuscript in response to this review.

Referee Comments 2 (Anonymous Referee):

This manuscript is an interesting one and I think it provide a more general method in calculating the barometric efficient (BE) in comparing with the provide Acworth's method. However, when reading this manuscript, I feel that there are several places that need to be made more clearly.

We thank the anonymous referee for the valuable time and constructive feedback.

In Equation (7) and Equation (10), the expression of Ac is different, it is very confused. Please explain why you use different expression for Ac. What's the difference between them.

We apologise for the confusion and will correct these definitions.

We have now checked and corrected Equations 7, 9 and 10 and revised Appendix A in response to this comment.

Line 187 please explain how you calculate the areial strain sensitivity.
We calculated this using *PyGTide* software (Rau, 2018) which is based on ETERNA 3.4 by Wenzel (1996). This was already mentioned in paragraphs 75 and 165 in the original manuscript.
We have added note of ETERNA (Wenzel, 1996) to the manuscript.

References:
Wenzel, H.-G. (1996). The nanogal software: Earth tide data processing package ETERNA 3.30. Bulletin d'Informations Mareés Terrestres, 124, 9425–9439.

Please provide a table to list all the parameters used in the example, and list all the result that obtained from your new method.
We will add such a table to the revised manuscript.
We have now added a new summary of the parameters that are calculated with our new method (Table 2).

Line 207 about the negative phase shift, the phase shift is very close to 0 (-1.1)° what about the error in the phase estimation? And there are always some inconsist between theoretical calculated and measured earth tide, how can you make sure that the -1.1° phase shift is real, not caused by the different in theoretical and measured one. Also, there are several recently publications that deal with the negative phase shift, which showed that the vertical flow across the aqutiard may also cause negative phases shift, and the effect of wellbore storage or skin effect can also cause negative or positive phase shift. I suggest you provide some discussion about it. Which you may also want to make some clarlity when discuss the indication of confinment during Line 216-226.
We will calculate the phase error and add additional discussion including appropriate references of the implications to the manuscript. This may have implications for the permeability and specific storage derived from Earth tides. However, it will not significantly affect the new BE estimation technique which is the focus of the manuscript.
In response to this comment, we have estimated the uncertainties from harmonic least-squares (HALS) including error propagation to amplitudes and phases as well as strain response and phase shift. The following specific changes were made to the manuscript:

- A new Appendix C was added explaining the uncertainty propagation from HALS (lines 325-330).
- Figure 3b was updated with horizontal and vertical error bars showing one standard deviation amplitude and phase uncertainties.
- Figure 5 was also updated by forward propagating the amplitude and phase uncertainties to arrive at K and Ss uncertainties.
- We added these uncertainties to the text in various places, e.g. lines 195.
- Where possible, we added the uncertainties to the new Table 2 (line 220).

We note that we are unable to determine if this small phase shift is real or not because we use theoretical earth tide strains. While this causes large uncertainties to the value of K, the uncertainties for Ss are very small. Further, the uncertainties are limited for lower K values possibly leading to a larger amplitude damping factor. We note that as the sensitivity of the phase difference between ET and GW to K drastically reduces in lower permeability settings, the confidence in results will increase. Conveniently, this is also the parameter range where the amplitude response is most affected giving confidence in the robustness of our new BE estimation approach. We have added this explanation to the discussion (lines 200).

We point out that our own assessment of a leaky vs completely confined system (compared in Figure 1) illustrates only negative phase shifts. The terms "wellbore storage" or "skin effect" appear exclusively in the BRF theory and are related to the water exchange between well and aquifer as controlled by the hydraulic conductivity. We are unsure of the exact criticism and providing further references for us to work with would help. We have tried to tighten the discussion in response to this comment, please refer to lines 210-215. Finally, we have fine-tuned the discussion about confinement and hope that this satisfies the reviewer's criticism. We note that since this is not the core topic of our manuscript we have pointed to the need for further research (lines 235 onwards).

Table 1 The unit of amplitude of ET is "m", thus many tidal components had amplitude more than 1 meter, are you sure?
These values are stated in Agnew (2010) and depict the amplitudes that are used to calculate Earth tide potentials. They do not represent a groundwater head response but serve to illustrate the relative magnitudes that can be expected for each frequency component. We will clarify this in our revised manuscript.
We have decided to delete this column from Table 1 because it does not contribute to the methodology outlined in the paper and it is somewhat misleading in our context.

Line 116-117 the authors argued that they assumed an aquitard with K=5.10-5 m/s, it is a rather permeabe, I think the aquitard should have a hydraulic conductivity with much small value.
We deliberately chose this value as a representative "worst case" for an aquitard. This discussion is meant to illustrate that fully confined conditions induce a tidal damping that is worse than under semi-confined conditions, i.e. a leaky aquitard. We will clarify this in our revisions.
To clarify this, we have added the following sentence to our manuscript: "*We used this value as a worst-case higher limit for an aquitard as the resulting amplitudes and phases provide a contrast from the confined case that is significant enough to see.*"

Line 120 Figure ?? which Figure do you mean.....
Apologies for the broken reference. This refers to Figure 1 and will be fixed.
We have corrected this internal reference in the revised manuscript.

Line 126 Equation 4.7 should be Equation 7
We will make this correction.
The hyphen refers to multiple equations from 4 through to 7. We did not see the need to make a response.

Line 134 Hsieh et al., 1988 should be Hsieh et al., 1987, and other places in the manuscript. "Hsieh, P. A., J. D. Bredehoeft, and J. M. Farr (1987), Determination of aquifer transmissivity from earth tide analysis, Water. Resour. Res., 23, 1824-1832."
Correct, we will carefully check and correct these references.
We have made multiple revisions to correct for the right references.

Code and data availability, I encourage the authors to share the code and data once the manuscript has been fully accepted.
We will make our dataset and code available if/when the manuscript is accepted.
We have made the dataset and code available on Figshare under: https://doi.org/10.6084/m9.figshare.11316281. We have noted this in the manuscript.

Author Response to the Public Discussion of "*Technical Note: Disentangling the groundwater response to Earth and atmospheric tides to improve subsurface characterisation*" by Gabriel C. Rau *et al.*

Referee Comments 3 (Anonymous Referee):

The paper by Gabriel C. Rau et al. with title: "Technical Note: Disentangling the groundwater response to Earth and atmospheric tides to improve subsurface characterization" presents an interesting study regarding the method to deal with the groundwater response to Earth and atmospheric tides. It seems to me that the approach for estimating barometric efficiency (BE) proposed in the manuscript is of particularly novelty. The study is well done and publication is recommended after the following concerns are addressed (moderate revision).

Many thanks for this positive review.

Major comments:

1. Page 4. Paragraph 4: Equation about the complex response to atmospheric tides alone shows some difference with that of Acworth et al., 2016. Phase shift between the Earth tide and barometric pressure was considered in Acworth et al., 2016. Why authors simplified this term? Please say something about this.

We did not simplify this term. In Acworth et al. (2016) we were not aware that there are more complicating factors to be considered when disentangling tidal influences. This awareness first came when analysing datasets with a strong Earth tide component and obtaining erroneous BE results when using our original method.

We had discussed the differences between Acworth et al. (2016) and this manuscript in several places within the original manuscript, for example see lines 29-45, lines 70-88, lines 94-97, lines 99-101 or lines 206-209. As this provides sufficient context, we do not see the need to make any further revisions.

2. Page 7. Paragraph 1: "In such cases, the concept of BE is no longer valid." The initial concept proposed by Jacob (1940) was that a change in groundwater head measured in a piezometer was directly proportional to the change in barometric pressure. BE value ranges from 0 to 1. BE=0 for an unconfined aquifer and BE=1 for an extreme ideal confined aquifer. Semi-confined conditions maybe belong to between such two extreme situations (e.g., a confined aquifer with a weakly permeable upper confining bed overlain by an unconfined aquifer). Why did authors consider it should be no longer valid in semi-confined conditions? Authors may wish to put some constraints or limitations.

May we point out that the relating BE to confinement is a misconception that often appears in the literature. The concept of BE quantifies the relative sharing of surface induced stress between liquid in the pores and the solid matrix which, by definition, only exists for semi-confined to confined conditions. It is therefore important to note that the value of BE is not indicative of confinement. For example, a clay system can have BE~0 (because clay is highly compressible) and still be fully confined. This is further explained in Turnadge et al. (2019) which is cited in the manuscript. To make this crystal clear, we will add some more clarifications to the manuscript during the revisions.

To address the criticism and avoid confusion, we have replaced the above sentence with the following: "*We note that the concept of BE describes a surface load sharing between matrix and pore water, which only exists under semi-confined to confined conditions, and that values of BE do not necessarily indicate the state of confinement \citep{Turnadge2019}.*" (lines 141-143).

3. Figure 3b and Figure 4: These two figures show some similarities. You may consider merging Figure 3b into Figure 4 and show more components in Figure 4.

We considered this in the original submission but decided against it for two reasons: (a) Figure 4 visualises the core of disentanglement (an non-intuitive methodology) based solely on the components M2 and S2, (b) any other components are not involved, adding them will distract from the clear message and overcrowd this figure

(i.e., make it much harder to understand the disentanglement). In the interest of showing all components we decided to add Figure 3b. Further, to explain the core method clearly and simply we decided to single out the relevant components in Figure 4. We wish to retain this communication strategy.
We do not see a need to revise the manuscript in response to this comment.

Minor comments:

1. Page 4. Paragraph 3: "The groundwater response to Earth tides only, for example at frequency M2, is assumed to be the same because the frequency is very close." Did you mean that M2 is assumed to be the same with S2? Please make it clearly.
We meant that the water level response to pore pressure at M2 and S2 should be the same because both frequencies are so close together. We will clarify this in our revisions.
We revised this sentence to read: "The groundwater response magnitude to Earth tides only, for example at frequency M_2 (1.93227 cpd), is assumed to be the same as for S_2 because the frequencies are very close."

2. Page 5 around Paragraph 2: "K=5*10-5 m/s" K should be changed as K'.
Thanks, we will make this change.
We have corrected this in the manuscript.

3. Page 5 Figure 1 highlights: "Figure ??" should be changed as Figure 1.
We will correct this mistake.
We have corrected this in the manuscript.

4. Equation (7) and Equation (10): Ac indicates the amplitude of pressure relationship between subsurface and well water level in Equation (7), however, in Equation (10) Ac indicates the amplitude of the well water level to an ET component. So, they are different in the physical aspect. It is easy to cause confusion if using the same symbol. Please replace one of them.
This is a mistake that we will rectify during the revisions.
We have already corrected this in the manuscript in response to RC1.

5. Page 7. last paragraph: Please add the value of the sampling frequency in this paragraph.
We will add this information during the revisions.
We have added the sentence: "*The dataset was sampled at 15-minute intervals (96 samples per day).*" (lines 166-167).

6. Page 8. last sentence in the last paragraph: Where is the Earth tide component M1? Please check it.
Thanks for spotting this mistake! We will carefully revise the figure to show all components.
We have now added details about the M1 Earth tide component to Table 1 and Figure 3.

7. Figure 3: Please make the label clearly in your Figure and avoid overlap of the label.
We will fix overlapping labels in the revised figure.
We have reformatted the labels in Figure 3 to comply with the text and improve readability.

8. Figure 3: The abbreviation of APES should be explained in the text or in the caption of the figure.
In the meantime, we have renamed this method to harmonic least-squares (HALS) and will revise and explain this abbreviation appropriately.

We have now added an explanation of HALS in the text (line 146).

Technical Note: Disentangling the groundwater response to Earth and atmospheric tides to improve subsurface characterisation

Gabriel C. Rau[1,2], Mark O. Cuthbert[3,2], R. Ian Acworth[2], and Philipp Blum[1]

[1]Karlsruhe Institute of Technology (KIT), Institute of Applied Geosciences (AGW), Karlsruhe, Germany
[2]The University of New South Wales (UNSW), Connected Waters Initiative Research Centre (CWI), Sydney, Australia
[3]Cardiff University, School of Earth and Ocean Sciences, Cardiff, United Kingdom

Correspondence: Gabriel C. Rau (gabriel.rau@kit.edu)

Abstract. The groundwater response to Earth tides and atmospheric pressure changes can be used to understand subsurface processes and estimate hydraulic and hydro-mechanical properties. We develop a generalised frequency domain approach to disentangle the impacts of Earth and atmospheric tides on groundwater level responses. By considering the complex harmonic properties of the signal, we improve upon a previous method for ~~estimating~~ quantifying barometric efficiency (BE) ~~estimation~~ while simultaneously assessing system confinement and estimating hydraulic conductivity as well as specific storage. We demonstrate and validate ~~the~~ this novel approach using an example barometric and groundwater pressure record with strong Earth tide influences. Our method enables improved and rapid assessment of subsurface processes and properties using standard pressure measurements.

1 Introduction

The groundwater response to barometric pressure and gravity changes caused by Earth tides have long been observed and are a powerful yet underutilised tool to passively characterise subsurface systems (McMillan et al., 2019). While atmospheric pressure changes act as a load on the subsurface and its groundwater pressure response can be related to compressible properties of the formation (e.g., Clark, 1967; Davis and Rasmussen, 1993), Earth tides cause areal strain resulting in small pore pressure changes (e.g., Bredehoeft, 1967; van der Kamp and Gale, 1983). The main research focus has long been the removal of both signals from the groundwater pressure in order to better understand and quantify processes such as pumping tests or recharge (e.g., Rojstaczer and Agnew, 1989). However, tidal forces are ubiquitous and their groundwater response can therefore also be utilised to quantify *in-situ* hydro-geomechanical properties (Allègre et al., 2016; Xue et al., 2016). Tidal harmonic components have long been named depending on their frequency (Agnew, 2010). A comprehensive list of the most common components found in groundwater head measurements are summarised in Table 1 (Merritt, 2004). McMillan et al. (2019) reviewed the state of the science, highlight the potential for such passive approaches and coin the term *Tidal Subsurface Analysis* (TSA).

Darwin name	Frequency [cpd]	~~ET Amplitude m~~ Barometric Pressure (BP)	Earth Tide (ET)	Groundwater (GW)
		Diurnal		
~~K_1~~ Q_1	~~1.002738~~ 0.893244	~~2.336899~~ -	yes	yes ~~yes~~
O_1	0.929536	~~0.546726~~ -	yes	yes
M_1	0.966446	-	yes	yes
P_1	0.997262	~~0.755110~~ yes	yes	yes
~~Q_1~~ S_1	~~0.893244~~ 1.000000	~~0.890820~~ yes	-	yes ~~yes~~
~~S_1~~ K_1	~~1.000000~~ 1.002738	yes	yes	~~-~~yes
		Semi-diurnal		
~~M_2~~ N_2	~~1.932274~~ 1.895982	~~4.287558~~ -	yes	yes
~~S_2~~ M_2	~~2.000000~~ 1.932274	~~1.968385~~ -	yes	yes ~~yes~~
~~N_2~~ S_2	~~1.895982~~ 2.000000	~~1.321448~~ yes	~~-~~yes	yes
K_2	2.005476	~~1.202015~~ yes	yes	yes

Table 1. ~~The nine~~ Overview of the major tidal components found in ~~groundwater~~ well water levels (Merritt, 2004; McMillan et al., 2019) grouped by mode (diurnal and semi-diurnal) and ordered ~~according to potential amplitude impact (Agnew, 2010)~~by frequency. Columns BP, ET and GW ~~identify the occurrence~~ show which component can occur in what type of ~~components~~record.

Cutillo and Bredehoeft (2011) analysed the groundwater response to both atmospheric pressure changes and Earth tides to quantify hydraulic and elastic properties. They reported that the frequency component S_2 of the groundwater response exhibits a reliable and strong response to Earth tides but could not be used because it is contaminated by atmospheric pressure influences. For this reason they concentrated their analysis on the Earth tide frequency M_2. Acworth and Brain (2008) and Acworth et al. (2015) used the groundwater response to atmospheric tides to estimate barometric efficiency, infer system confinement and calculate compressible storage. They used the tide frequency S_2 in their work but did not take account of the effects of the phase lags between the earth tide, atmospheric and groundwater tides that have been found to introduce errors in the analysis for higher levels of barometric efficiency.

Acworth et al. (2016) published a method which objectively quantifies barometric efficiency (BE) using the groundwater response to atmospheric tides. Their approach considered the impact of phase lags between S_2^{AT} and S_2^{ET} in the amplitude response of the groundwater system. Their work demonstrated that: (1) the harmonic addition theorem could be used to quantitatively disentangle the groundwater response to both Earth and atmospheric tides (EAT) acting at the same frequency, (2) a theoretical Earth tide record is sufficient for this purpose. Because Earth tide records can be calculated with very high accuracy for any location on Earth and time periods of general interest (e.g., McMillan et al., 2019), this has opened the door for the widespread use of common barometric and groundwater pressure measurements (the latter in the form of standard well water levels) to characterise and quantify groundwater systems with little effort. Turnadge et al. (2019) compared different BE estimation methods and concluded that Acworth et al. (2016) delivers robust results.

The method by Acworth et al. (2016) is based on the assumptions that the borehole water level is representative of subsurface pore pressure, i.e. there is an instantaneous and undamped response. Under such conditions, only the phase difference between the theoretical Earth and atmospheric tide drivers is required to correct the groundwater response amplitude. However, it has been established that the well water level response to Earth tide forces also depends on hydraulic properties of the aquifer and well geometry ~~(Bredehoeft, 1967; Gieske and De Vries, 1985; Hsieh et al., 1988)~~ (Bredehoeft, 1967; Gieske and De Vries, 1985; Hsieh et as well as vadose zone air transport for conditions that are not confined (Rojstaczer, 1988; Allègre et al., 2016; Xue et al., 2016). In fact, the amplitude and phase responses to Earth tides embedded in well water levels have been used to quantify subsurface hydraulic properties ~~(e.g., Hsieh et al., 1988; Ritzi et al., 1991; Xue et al., 2016). Hsieh et al. (1988)~~ (e.g., Hsieh et al., 1987; Ritzi et al., 19 . Hsieh et al. (1987) reports an average phase shift of -12° between the M_2 Earth tide potential and its well water level response. Consequently, an instantaneous and undamped groundwater response to Earth tides is not always a given and phase delays must be also considered when quantifying ~~BE~~ BE_{S_2} from the groundwater response to atmospheric tides.

In this technical note we generalise the method by Acworth et al. (2016) by more completely disentangling the groundwater response to EAT in the frequency domain. We then illustrate the interpretative value of this new approach using an example atmospheric pressure and borehole water level record that is strongly affected by EAT followed by verifying our results using the well's barometric response function calculated in the time domain.

2 A generalised frequency-domain method

2.1 Complete tidal disentanglement

Since the extension of the method published in Acworth et al. (2016) to a generalised approach requires consideration of both the amplitudes and phases, we use complex numbers (denoted with a hat) for improved clarity. The complex numbers can be expressed with their real and imaginary components as

$$\hat{z}_c = a_c + b_c i = A_c e^{i\Phi_c} \tag{1}$$

where a_c and b_c are the real and imaginary parts, respectively; $i = \sqrt{-1}$ following standard definition. The complex coefficients are related to harmonic amplitudes and phases as

$$A_c = \mathrm{abs}(\hat{z}_c) = \sqrt{a_c^2 + b_c^2} \tag{2}$$

and

$$\Phi_c = \arg(\hat{z}_c) = \arg \frac{b_c}{a_c} \left[\frac{a_c}{b_c} \right], \tag{3}$$

where the results within $-\pi \leq \Phi_c \leq \pi$.

Throughout this manuscript, subscripts refer to the considered tidal components c, i.e. M_2 (1.93227 cpd) and S_2 (2 cpd). Superscripts stand for the measured parameter, i.e. GW stands for groundwater pressure head (measured as borehole water

level and generally only required as a relative measurement), AT is atmospheric pressure (as water head equivalent) and ET is Earth tide (here, we use strain). Importantly, $GW.ET$ and $GW.AT$ represent the disentangled groundwater components response to Earth and atmospheric tides, respectively.

The method by Acworth et al. (2016) can be generalised to allow complete disentanglement of Earth and atmospheric tide influences from the groundwater response as follows:

1. The complex groundwater response to the Earth tide only driver for the M_2 (1.93227 cpd) component is compared to the complex, theoretical Earth tide generated for the well geo-location, time and duration. Theoretical Earth tides can be ~~synthesised~~ calculated using software packages such as *ETERNA* (Wenzel, 1996), *PyGTide* (Rau, 2018) (which utilises the latest tidal catalogue), *Baytap08* (Agnew, 2008) or *TSoft* (Van Camp and Vauterin, 2005) (which was originally designed to analyse gravity records). Records for the theoretical Earth tide potential or gravity variations are highly accurate and avoid the need for measurements (McMillan et al., 2019).

2. For some tidal components, for example S_2 (2.0 cpd), the well water level responds to both Earth and atmospheric tides. The groundwater response magnitude to Earth tides only, for example at frequency M_2 (1.93227 cpd), is assumed to be the same ~~because the frequency is~~ as for S_2 because the frequencies are very close. Consequently, the S_2 groundwater response to Earth tides alone can be calculated using

$$\hat{z}_{S_2}^{GW.ET} = \frac{\hat{z}_{M_2}^{GW}}{\hat{z}_{M_2}^{ET}} \hat{z}_{S_2}^{ET}. \tag{4}$$

3. Since the measured well water level response for S_2 contains a harmonic combination of both Earth and atmospheric tides (McMillan et al., 2019)

$$\hat{z}_{S_2}^{GW} = \hat{z}_{S_2}^{GW.ET} + \hat{z}_{S_2}^{GW.AT}, \tag{5}$$

the complex response to atmospheric tides alone can be calculated as

$$\hat{z}_{S_2}^{GW.AT} = \hat{z}_{S_2}^{GW} - \hat{z}_{S_2}^{GW.ET} = \hat{z}_{S_2}^{GW} - \frac{\hat{z}_{M_2}^{GW}}{\hat{z}_{M_2}^{ET}} \hat{z}_{S_2}^{ET}. \tag{6}$$

Unfortunately, Equation 6 does not have a simplified expression consisting only of real-valued numbers or functions.

It is important to note that our extended approach given in Equations 4-6 is correct irrespective of any processes that may affect the subsurface strain response to the stress induced by Earth tides. For example, delays may result from the physical characteristics of the aquifer borehole system but will be very similar for M_2 and S_2 because the frequencies are so close together. The theoretical Earth tide record merely helps to determine the absolute amplitudes and phases of the Earth tide response at S_2 by accounting for the differences between the complex M_2 and S_2 determined from the theoretical Earth tide record to the absolute one at M_2 measured in the well. The approach extends the method developed by Acworth et al. (2016) because it considers all the signal phases in addition to their amplitudes. Since the inference of the well response to Earth tides is relative, the disentanglement can be done with any theoretical Earth tide signal, e.g. potentials, gravity variations or estimated strains.

2.2 Relationship between borehole water levels and subsurface pore pressure

Acworth et al. (2016) assumed that the groundwater pressure head (i.e., the well water level) is representative of the subsurface pore pressure, i.e. an instantaneous and undamped response. However, calculation of the true BE based on subsurface pore pressure (outside of the well screen) requires a closer look at this relationship. Since tidal components comply well with harmonic functions, we can invoke the assumption that there is harmonically varying flow between the formation and the well ~~(e.g., Bredehoeft, 1967; Hsieh et al., 1988; Rojstaczer, 1988)~~(e.g., Bredehoeft, 1967; Hsieh et al., 1987; Rojstaczer, 1988). This groundwater flow problem has been solved analytically for confined ~~(Hsieh et al., 1988)~~ (Hsieh et al., 1987) and semi-confined (i.e. situations with vertical leakage through an overlying aquitard) (Rojstaczer, 1988) conditions (see Appendix ??A). For the pressure relationship between subsurface and well water level, an amplitude ratio can be defined as

$$A^r{}_c = \mathrm{abs}\,\frac{\hat{z}_c^{GW}}{\hat{z}_c^{SP}}\left[\frac{\hat{z}_c^{GW}}{\hat{z}_c^{PP}}\right] = \mathrm{abs}\left[\hat{H}(f_c, T, S, r_{wc}, r_{ws})\right]. \tag{7}$$

Further, a phase shift can be formulated as

$$\Delta\phi_c = \arg\frac{\hat{z}_c^{GW}}{\hat{z}_c^{SP}}\left[\frac{\hat{z}_c^{GW}}{\hat{z}_c^{PP}}\right] = \arg\left[\hat{H}(f_c, T, S, r_{wc}, r_{ws})\right]. \tag{8}$$

Here, the subscript c depicts any tidal component with distinct frequency; superscripts GW and ~~SP~~ PP stand for well water level~~and~~, subsurface pore pressure, respectively. The complex analytical function $\hat{H}$ is given in Appendix ~~??~~ A and depends on the variables r_{wc} and r_{ws} which are the radius of the well casing and screen, respectively, b is the screen length; $T = K \cdot b$ and $S = S_s \cdot b$ are the transmissivity and storativity of the formation located along the well screen ~~(Hsieh et al., 1988)~~ (Hsieh et al., 1987).

Figure 1 shows the amplitude ratio and phase shift calculated for the M_2 Earth tide component (1.93227 cpd) and a hypothetical groundwater observation point with radius of 25 mm and screen length of 1 m. For the leaky aquifer solution we assumed an aquitard with ~~$K = 5 \cdot 10^{-5}$~~ $K' = 5 \cdot 10^{-5}$ m/s and vertical thickness of 2 m. We used this value as a worst-case higher limit for an aquitard as the resulting amplitudes and phases provide a contrast from the confined case that is significant enough to visualise. The solutions illustrate that there is a frequency dependent damping and phase shift in the well water level response to the aquifer pore pressure. Importantly, Figure 1 highlights the following:

- the strongest modification of the harmonic response occurs for fully confined and not for leaky conditions (Figure ??1);
- both amplitude damping and phase shifts are mainly controlled by the subsurface hydraulic conductivity. For the confined case, ~~$A > 0.99$~~ $A^r_{S_s} > 0.99$ which means that the relative error is smaller than 1% for $K > 1 \cdot 10^{-5}$ m/s and therefore negligible. However, A dramatically decreases ~~in~~ under lower hydraulic conductivity conditions and must therefore be considered for ~~BE~~ BE^{AT} estimations;
- S_s does not significantly affect the well water level response, especially for $K > 1 \cdot 10^{-5}$ m/s. However, the amplitude response to the Earth tide strain is proportional to S_s (Equation 7).

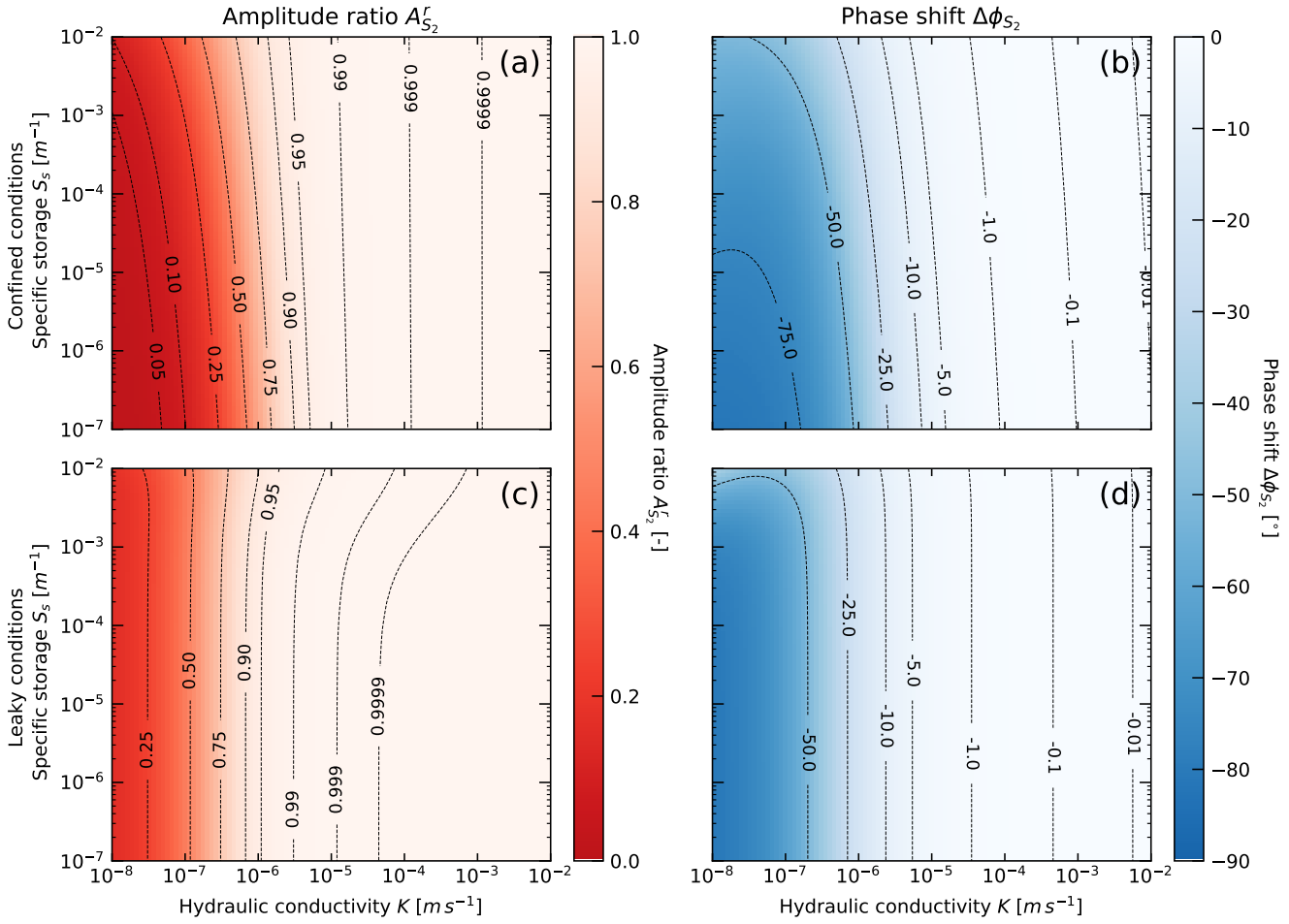

Figure 1. Amplitude ratio and phase shift relationship between subsurface pore pressure and well water level for harmonic forcing under fully confined (a and b) as well as conditions of vertical water leakage under semi-confined conditions (c and d; the leaky aquitard has $K' = 5 \cdot 10^{-5}$ m/s and $b' = 2$ m). The plots are calculated for a hypothetical well with radius of 25 mm and screen length of 1 m and realistic ranges of hydraulic conductivity and specific storage.

Using Equations 4-7, a generalised method for objective ~~BE~~ BE^{AT} quantification using the groundwater response to atmospheric tides~~(~~, for example at S_2~~)~~, can be formulated as follows

$$BE^{AT}_{S_2} = \frac{1}{A_c} \frac{1}{A^r_{S_2}} \operatorname{abs} \frac{\hat{z}^{GW.AT}_c}{\hat{z}^{AT}_c} \left[\frac{\hat{z}^{GW.AT}_{S_2}}{\hat{z}^{AT}_{S_2}} \right]. \tag{9}$$

Here, ~~A_c~~ $A^r_{S_2}$ accounts for the damping introduced by the subsurface-well system under conditions of low hydraulic conductivity. Due to the closeness of the S_2 and the M_2 frequencies we can assume that $A^r_{S_2} \approx A^r_{M_2}$.

The tidal disentanglement further enables estimation of the subsurface hydraulic conductivity (K) and specific storage (S_s) using the water level response to Earth tides. A negative phase shift between M_2 and its groundwater response (well water level lags the Earth tide strain) requires horizontal flow in and out of the well and is therefore indicative of confined conditions (Roeloffs et al., 1989; Allègre et al., 2016; Xue et al., 2016). In this case, the amplitude and phase response of the well water level to an ET strain component is related by ~~(Hsieh et al., 1988)~~ (Allègre et al., 2016; Xue et al., 2016)

$$A^{e}_{c\,M_2} = \frac{1}{S_s}\,\mathrm{abs}\,\frac{\hat{z}^{GW}_{c}}{\hat{z}^{SP}_{c}}\left[\frac{\hat{z}^{GW}_{M_2}}{\hat{z}^{ET}_{M_2}}\right] = \frac{A^{r}_{M_2}}{S_s} \tag{10}$$

(aerial strain sensitivity, equivalent to Equation A12 in Appendix ~~??) and~~ A) and

$$\Delta\phi_{c\,M_2} = \arg\frac{\hat{z}^{GW}_{c}}{\hat{z}^{SP}_{c}}\left[\frac{\hat{z}^{GW}_{M_2}}{\hat{z}^{ET}_{M_2}}\right] \tag{11}$$

(equivalent to Equation A13 in Appendix ??A). A positive phase shift is indicative of vertical water movement and semi-confined conditions (Roeloffs et al., 1989; Xue et al., 2016). ~~In such cases,~~ We note that the concept of BE ~~is no longer valid~~describes a surface load sharing between matrix and pore water, which only exists under semi-confined to confined conditions, and that values of BE do not necessarily indicate the state of confinement (Turnadge et al., 2019).

2.3 Extraction of tidal components using harmonic least-squares

The first step towards tidal disentanglement is to extract the tidal harmonics from the time series. Since the frequencies of the main tidal components are well known (e.g., McMillan et al., 2019), a ~~general~~ harmonic least-squares (HALS) estimation can be applied as follows (Agnew, 2010)

$$\min_{a_c,b_c}\sum_{n=0}^{N}{}_{n=1}^{N}\left[y_n(t_n) - \sum_{c=0}^{C}{}_{c=1}\left[a_c\cos(2\pi f_c t_n) + b_c\sin(2\pi f_c t_n)\right]\right]^2. \tag{12}$$

Here, N is the number of discrete samples, $y_n(t_n)$ is the sample value at time t_n, C is the total number of tidal components c with frequency f_c. Table 1 shows the nine strongest tidal components that are generally observable in groundwater pressure measurements (Merritt, 2004; McMillan et al., 2019) and are required for finding the best fit using Equation ??12. The coefficients a_c and b_c from Equation ~~??~~ 12 serve to derive the complex numbers representing each tidal constituent using Equation 1. We further calculate the uncertainties of amplitudes and phases by propagating the covariances obtained from HALS fitting (Equation 12) using Equations 2 and 3. For details refer to Appendix C.

Before extracting tidal harmonics, lower frequency variations should be removed. We suggest to first apply de-trending filter with a cut-off frequency of $f < 0.5$ cpd. This improves the least-squares approximation. It is important to note that the components used in the regression have to be customised for barometric pressure (BP), Earth tides (ET) and groundwater pressure head (GW) according to this table. For example, S_1 is only contained in BP. This list is based on the findings by Merritt (2004) and McMillan et al. (2019).

3 Application

The three ~~*BE*~~ BE^{AT} examples illustrated in Acworth et al. (2016) show a limited impact of Earth tides relative to those of the atmospheric tides resulting in a small magnitude correction at S_2. To illustrate our new tidal disentanglement approach, we deliberately use a well water level record in which the Earth tide influence exceeds that of the atmospheric tides. This record originates from the well BLM-1 in Death Valley (California, USA; WGS84 longitude: -116.471360°, latitude: 36.408130°, height: 688 m; casing and screen radius: 0.127 m, screen length: 106 m) which provided data for a previous analysis (Cutillo and Bredehoeft, 2011). The dataset used here was recorded in the same well but at a later time. The dataset was sampled at 15-minute intervals (96 samples per day).

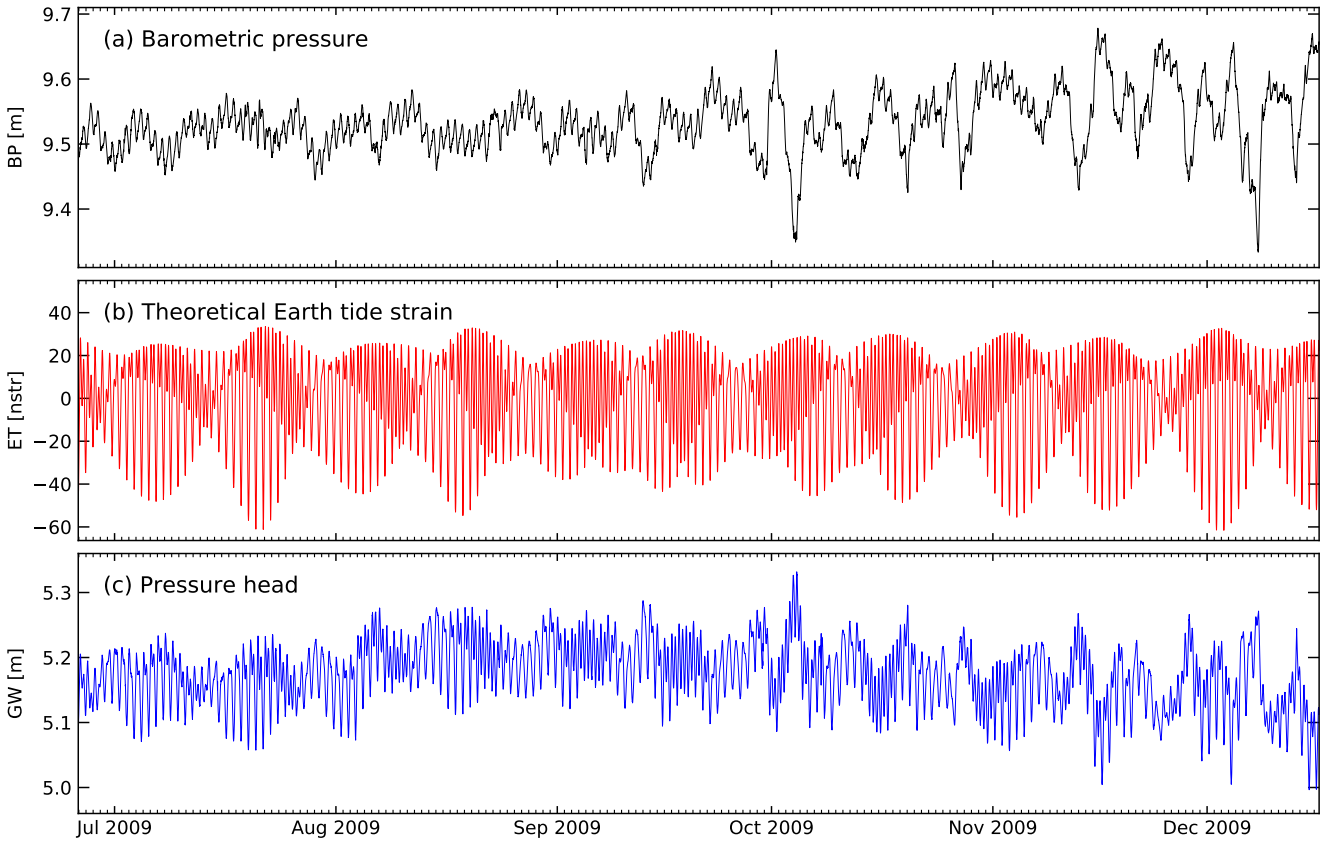

Figure 2. Time series of (a) barometric pressure (BP) (b) Theoretical Earth tide strains (ET) were calculated for the same duration and sampling rate and the well's geo-location using *PyGTide* (Rau, 2018) and (c) well water levels (GW) as measured in the well BLM-1 in Death Valley (California, USA). The vertical axes for BP and GW are limited to the same range for a visual comparison.

Figure 2 shows the barometric pressure (BP; black line, converted to pressure head equivalent), groundwater pressure head (GW; blue line, as measured in the well) and Earth tide strains (ET; red line) for BLM-1 over a time period of almost six months

(25 June 2009 to 16 December 2009). The Earth tide strains were calculated using the Python package *PyGTide* (Rau, 2018) for the same time period and sampling frequency as the pressure measurements. It is interesting to note that both Earth tide and atmospheric pressure signatures are clearly visible in the groundwater response. In fact, the impact of both atmospheric pressure and Earth tide strains on the borehole water level is obvious just by looking at the raw dataset.

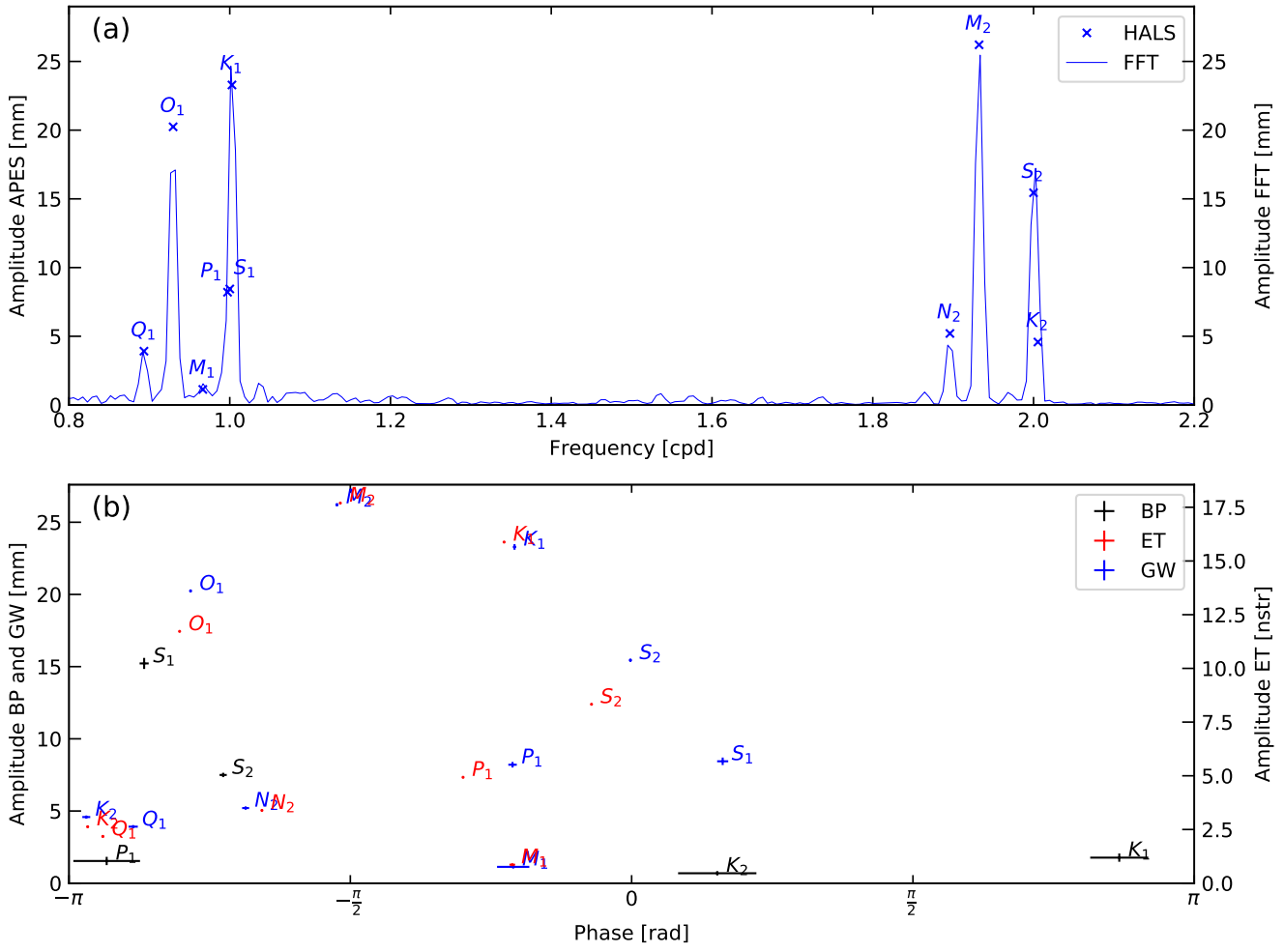

Figure 3. (a) A comparison of groundwater (GW) amplitudes for the interval $0.8 \leq f \leq 2.2$ cpd derived using the general harmonic least-squares estimation (Equation ??12) and the standard *Fast Fourier Transform*. (b) Amplitudes and phases of the most common tidal components in groundwater (GW), barometric pressure (BP) and Earth tides (ET) determined using harmonic least-squares estimation. Note that horizontal and vertical error bars show the uncertainty of one standard deviation (Appendix C).

As a next step we extracted the tidal harmonic components from all three time series (BP, ET and GW in Figure 2) using the harmonic least-squares estimation approach described in Section ??. Figure ??2.3. Figure 3a shows the estimated amplitudes of the tidal components compared to a Fourier amplitude spectrum of the groundwater record. This example illustrates that

separating tidal components with close-by frequencies is a clear challenge for the Fourier transform even when the record duration is longer than that recommended by Acworth et al. (2016). It further highlights the well-known fact that spectral leakage can lead to errors in estimating the properties of the harmonic components (e.g., Tary et al., 2014).

Figure ??3b maps the amplitudes of the ~~ten tidal components~~ tidal components (Table 1) extracted from the original time series depicted in Figure 2 against their phases. As expected, the strongest impact stems from the Earth tide only component M_2. It is interesting to observe the similarity in the groundwater response magnitudes for all other Earth tide components, e.g. K_1, O_1, N_2, Q_1, M_1 (in decreasing order of impact). It is apparent that at frequencies for which the groundwater record is influenced by both Earth and atmospheric tides, there is a substantial misalignment in amplitudes and phases of these components in groundwater in comparison to the forcing signals, e.g. see S_2 or S_1.

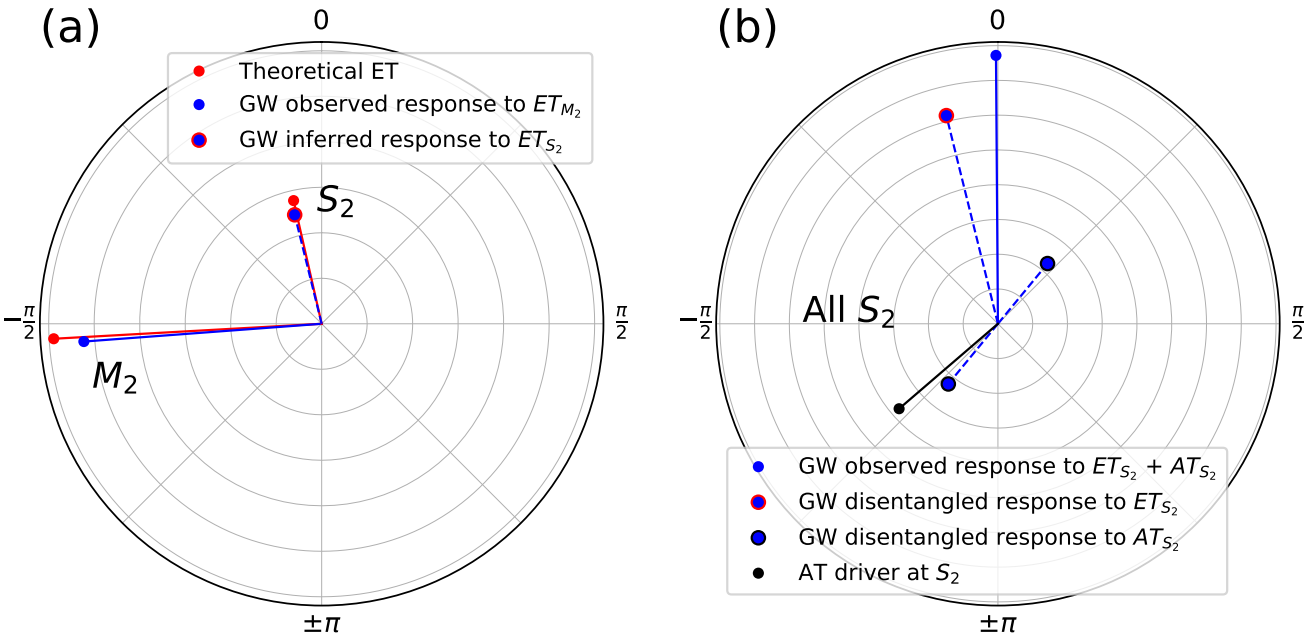

Figure 4. Polar plots showing amplitudes and phases derived from the fitting coefficients using Equations 1-3. (a) Results of the complex inference of the well response to Earth tides at S_2 from the response at M_2 (Equation 4). (b) Harmonic disentanglement of the well response to atmospheric tides at S_2 (Equation 6). In (a) the Earth tide magnitude is scaled to improve comparison with the groundwater response.

To illustrate the tidal disentanglement, we use polar plots to visualise the key components. Figure 4a shows the amplitude and phase of the M_2 component present in ET and GW. We apply the approach developed in Section 2.1 to infer the S_2 response in the well that is caused by the Earth tides alone using the theoretical Earth tide strains (note that the ET magnitude is scaled to improve comparison). Figure 4b shows the atmospheric tide driver at S_2, the combined well water level response to EAT, the inferred groundwater response to S_2 as well as the disentangled S_2 response to atmospheric tides. All parameters and uncertainties calculated in this work are summarised in Table 2.

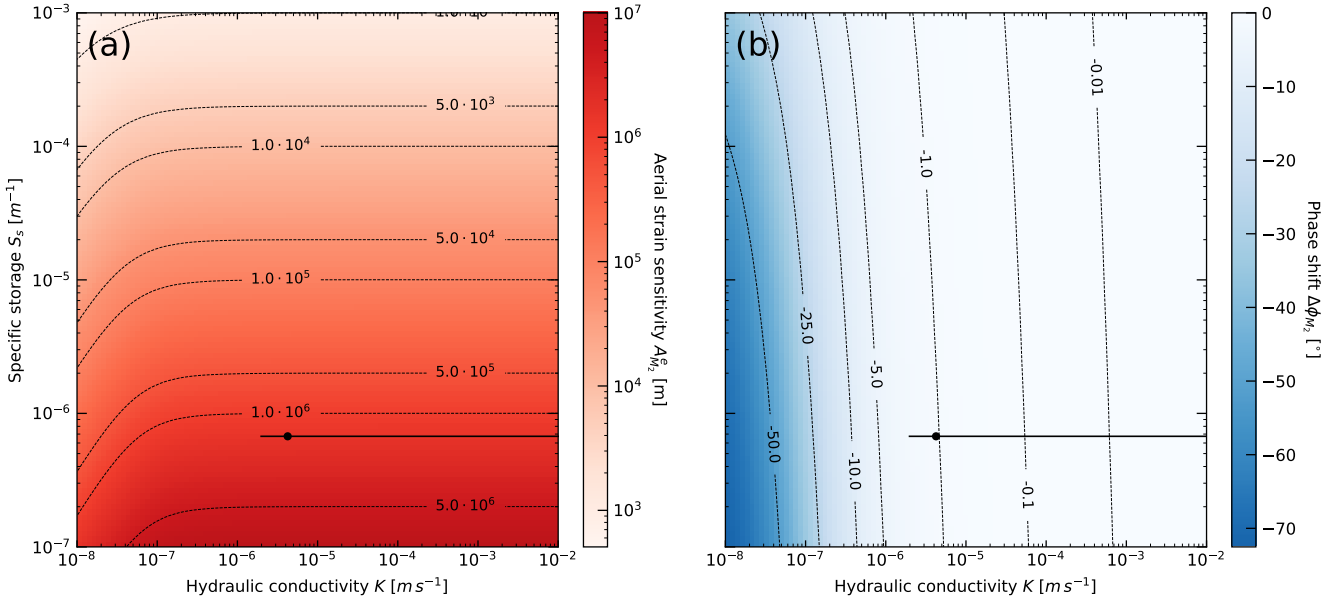

Figure 5. Well water level response to pore pressure for BLM-1 (well radius of 0.127 m and length of 106 m) and S_2 frequency (2.0 cpd). Black dots represent the results for this well found by least-squares fitting of the amplitude and phase response to the analytical solutions by ~~Hsieh et al. (1988)~~Hsieh et al. (1987). The horizontal and vertical (not visible) black lines depict the property ranges as a result of uncertainties in the aerial strain sensitivity and phase difference.

To account for the amplitude damping and phase shifting of the well in response to the harmonic pore pressure changes, we have used the dimensions of the well BLM-1 (see earlier) to calculate the solution space of the analytical solution for confined conditions (Appendix ~~??~~A) for the M_2 frequency as well as for realistic limits of hydraulic conductivity ($1{\cdot}10^{-8} < K < 1{\cdot}10^{-2}$ m/s) and specific storage ($1{\cdot}10^{-7} < S_s < 1{\cdot}10^{-3}$ 1/m). The aerial strain sensitivity and phase shift between Earth tides and well response to M_2 is shown in Figure 5. We further used ~~this~~ Equations 10 and 11 to estimate the ~~average hydraulic conductivity~~ hydraulic conductivity as $K \approx 4.2 \cdot 10^{-6}$ m/s (ranging from $2.0 \cdot 10^{-6}$ to impossibly high values) and specific storage ~~of~~ as $S_s \approx 6.7 \cdot 10^{-7}$ 1/m (ranging from $6.69 \cdot 10^{-7}$ to $6.77 \cdot 10^{-7}$ 1/m) representative for the materials along the well screen from the groundwater response to Earth tides ~~as $K \sim 4.2 \cdot 10^{-6}$ m/s and $S_s \sim 6.7 \cdot 10^{-7}$ 1/m (see black dots~~ (note the black annotations in Figure 5)~~using Equations 10 and 11~~. The S_s falls within the poroelastic limits determined by (Rau et al., 2018).

The damping of the amplitude in the well in this case is only $A^r_{M_2} \approx 0.998$, which differs to the aquifer pore pressure by merely $\approx 0.2\%$. It is important to note ~~that the value of K is prone to significant uncertainties since Equation 11 is very sensitive to~~ the high sensitivity to phase differences, i.e. small changes in ~~phase (Figure 5~~Δphi_{M_2} can cause large changes in the value of K (Equation A13 and Figure 5b). However, we note that as the sensitivity of the phase difference $\Delta\phi_{M_2}$ to K drastically reduces in lower permeability settings (Figure 1b), the ~~damping of the amplitude by the well in this case is only $A = 0.998$, which differs to the pore pressure by merely $\sim 0.2\%$. This is likely smaller than possible errors resulting from the harmonic~~

~~regression and illustrates that the well water level is a good representation of the aquifer pore pressure in this case~~confidence in K values will increase. Conveniently, this is also the value range where the amplitude response is most affected (Figure 1a) allowing confidence in the robustness of our new BE_{S_2} estimation approach for the investigated property ranges.

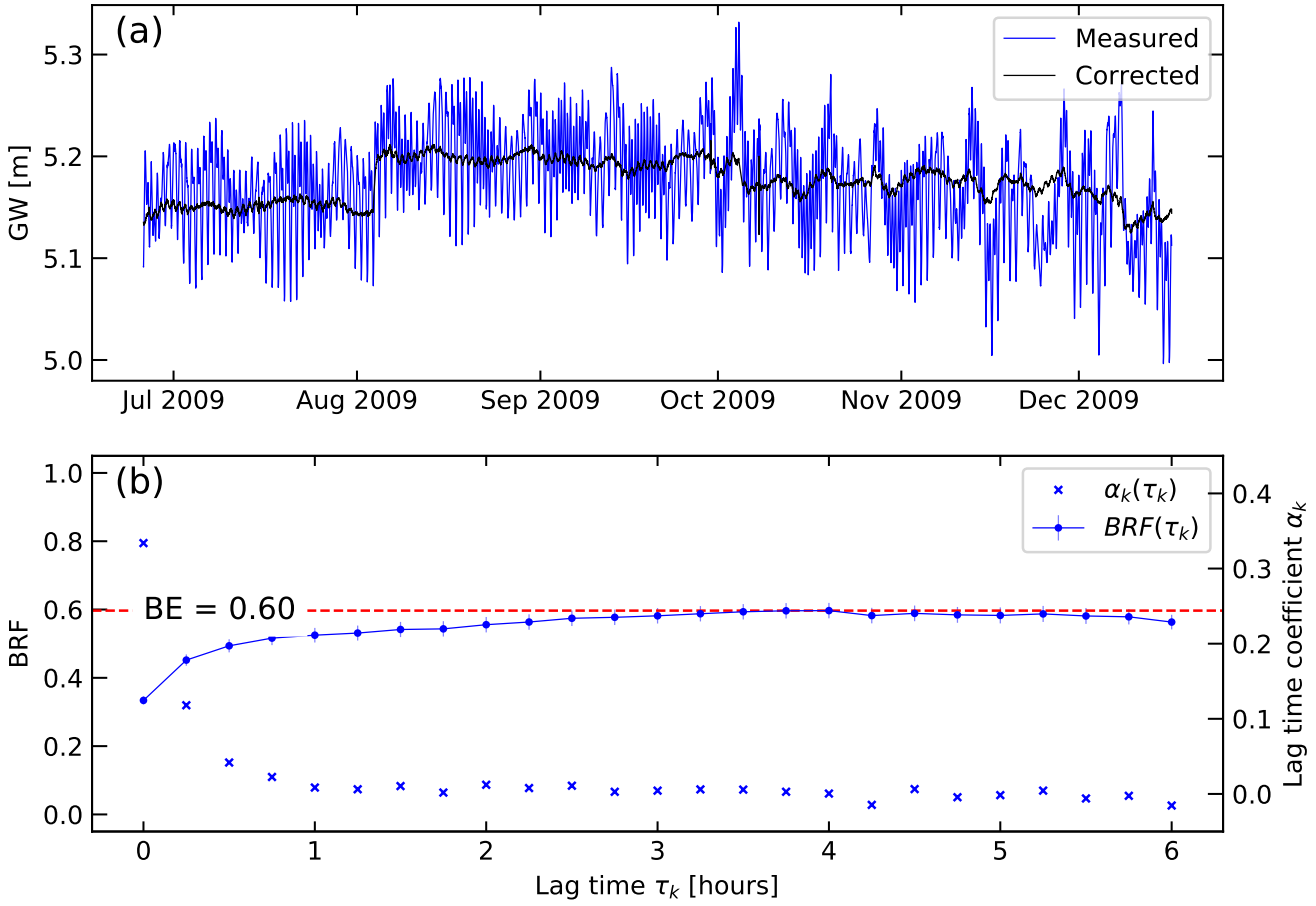

Figure 6. (a) Borehole pressure head (GW) measured and corrected for barometric and Earth tide influences. (b) Barometric response function (~~BRF~~BRF) and ~~BE~~ BE_{BRF} calculated using the records shown in Figure 2 and the approach summarised in Appendix B.

Using Equation 9, we calculate a ~~$BE = 0.60$~~ $BE_{S_2} = 0.60$ from the disentangled groundwater response to atmospheric tides at S_2 frequency. This is significantly different to the ~~$BE = 1.29$~~ $BE_{S_2} = 1.29$ that results from using the method by Acworth et al. (2016). The latter is clearly erroneous, since it is larger than 1, owing to the limited phase correction and leading to an incomplete disentanglement of the the groundwater response to EAT. To verify our results, we independently calculated ~~BE for this dataset~~ BE_{BRF} for this location using the well established Barometric Response Function (~~BRF~~BRF) approach developed and illustrated ~~by others~~ previously (a brief summary of the theory is given in Appendix B) (Rasmussen and Crawford, 1997; Spane, 2002; Toll and Rasmussen, 2007; Butler et al., 2011). The ~~result indicates that BLM-1 is screened~~

~~in a confined system that responds to barometric pressure with a typical exponential delay~~ asymptotic value of the BRF at larger delay times represents confined conditions. The results further exhibit an exponential increase of the BRF over lag time (Figure 6b). ~~The BRF-based $BE \sim 0.60$~~ This is typical for water exchange controlled by the subsurface hydraulic conductivity where the shorter the lag time the stronger the deviation from BE (Rasmussen and Crawford, 1997), and it complies well with the frequency dependent relationship shown in Figure 1 (Rojstaczer, 1988; Rojstaczer and Agnew, 1989).

The BRF-based $BE_{BRF} \approx 0.60$ exactly matches that calculated using Equation 9 confirming the robustness of the tidal disentanglement methodology we present ~~here. The BRF~~ in this work. The BRF is able to adequately remove the Earth and atmospheric influences on the measured groundwater ~~level~~ levels (Figure 6a). While ~~BRFs~~ BRFs are capable of indicating system confinement and estimating BE, they have not been ~~illustrated useful~~ used for estimating hydraulic properties.

The negative phase shift between Earth tides and groundwater pressure ($\Delta\phi_{M_2}^{GW.ET} = -1.1°$, see Figure 4a) can be interpreted as horizontal flow between the subsurface and the well which occurs under confined conditions (Roeloffs et al., 1989; Xue et al., 2016). Confined conditions can also be interpreted from the fact that the ~~BRF-time~~ BRF-time values reach a maximum value that is representative of the BE (Rasmussen and Crawford, 1997). Since this means that the well is screened in the confined zone, vertical loading due to atmospheric tides should also predominantly induce horizontal flow between the subsurface and the well with the same phase difference as that in response to Earth tides but considering the typical 180° (Figure 4b) difference related to the subsurface stress balance (Rojstaczer, 1988; Acworth et al., 2016). In fact, $\Delta\phi_{S_2}^{GW.AT} = -9.8°$ which is also negative and very close to the phase delay in response to Earth tides. ~~This phase difference explains the initial increase in BRF values reflecting a small delay in the well response to barometric pressure changes.~~

Previous works have reported that a phase difference of 180° between the atmospheric tides and the groundwater response at S_2 can be used to indicate confinement (Acworth et al., 2016, 2017). However, this did not consider the fully disentangled groundwater response to atmospheric tides. Further, Rojstaczer (1988) has illustrated that the well response to barometric pressure depends on a number of processes accounting for the pressure propagation between surface and well resulting in a frequency dependent response of the borehole water level to barometric forcing. We propose that a combination of $\Delta\phi_{M_2}$ and $\Delta\phi_{S_2}$ could be diagnostic of the subsurface conditions at the borehole location. For example, a negative $\Delta\phi_{M_2}$ is indicative of ~~the~~ horizontal flow occurring under confined conditions for which $\Delta\phi_{S_2}$ should ~~be exactly~~ equally be shifted accounting for the 180° ~~out of phase~~ phase difference. A positive $\Delta\phi_{M_2}$ has been attributed to vertical water movement (Hanson and Owen, 1982; Roeloffs et al., 1989; Xue et al., 2016) under which the response of $\Delta\phi_{S_2}$ could become diagnostic of the vertical pressure propagation and vadose zone properties (Rojstaczer, 1988). However, further research is required to develop a robust approach for detecting confinement status at a particular frequency.

4 Conclusions

We present a frequency domain method to disentangle the groundwater response to Earth and atmospheric tides. It is a more general solution than that previously presented by Acworth et al. (2016) since it is also applicable to subsurface environments with lower hydraulic conductivities, where measurable damping and time lags between formation pressure changes and well

Parameter	Value	Uncertainty ($\pm\sigma$) or range	Unit
$A^{ET}_{M_2}$	17.7	$\pm$ 0.01	nstr
$\phi^{ET}_{M_2}$	-93.2	$\pm$ 0.04	°
$A^{ET}_{S_2}$	8.3	$\pm$ 0.01	nstr
$\phi^{ET}_{S_2}$	-12.84	$\pm$ 0.09	°
$A^{AT}_{S_2}$	7.5	$\pm$ 0.2	mm
$\phi^{AT}_{S_2}$	-130.68	$\pm$ 1.15	°
$A^{GW}_{M_2}$	26.2	$\pm$ 0.1	mm
$\phi^{GW}_{M_2}$	-94.28	$\pm$ 0.22	°
$A^{GW}_{S_2}$	15.4	$\pm$ 0.1	mm
$\phi^{GW}_{S_2}$	-0.4	$\pm$ 0.38	°
$A^{GW.ET}_{S_2}$	12.3		mm
$\phi^{GW.ET}_{S_2}$	-13.92		°
$A^{GW.AT}_{S_2}$	4.5		mm
$\phi^{GW.AT}_{S_2}$	39.54		°
$A^{e}_{M_2}$	1,481,243	$\pm$ 5,739	m
$A^{r}_{M_2}$ and $A^{r}_{S_2}$	0.998		
$\Delta\phi^{GW.ET}_{M_2}$	-1.08	$\pm$ 1.12	°
K	$4.20 \cdot 10^{-6}$	$2.0 \cdot 10^{-6} < K < \infty$	m/s
S_s	$6.72 \cdot 10^{-7}$	$6.69 \cdot 10^{-7} < S_s < 6.77 \cdot 10^{-7}$	1/m
$BE^{AT}_{S_2}$	0.6		
BE_{BRF}	0.6		

Table 2. Summary of the parameters, values and uncertainties calculated in this work.

water level responses may be present. The approach only requires simultaneous records of barometric and groundwater pressure head in combination with theoretical Earth tide potential, gravity or strain variations which are either standard measurements or can readily be calculated for any borehole geo-position using readily available software. Our novel approach exploits the fact that the complex harmonic components can be determined for each variable, i.e. barometric pressure, borehole water level and Earth tides from which subsurface flow direction (horizontal vs. vertical) in response to stresses allow inference

of confinement, estimation of barometric efficiency (BE), hydraulic conductivity as well as specific storage. We show that BE calculation using the borehole water level response to atmospheric tides may be substantially influenced by the hydraulic conductivity of the materials surrounding the well screen where $K < 1 \cdot 10^{-5}$ m/s.

Our method enables improved and rapid estimation of BE in general but especially for cases where the borehole water level is strongly influenced by Earth tides. Under such conditions, the influence of the phase difference between Earth tides and its groundwater response has to be also considered when revealing the atmospheric tide embedded in the S_2 component of groundwater head measurements. The generalised solution further improves existing approaches and provides a next step towards more reliable quantification of subsurface hydro-geomechanical properties using the groundwater response to Earth and atmospheric tides McMillan et al. (2019).

Code and data availability. The code and dataset are available on Figshare under https://doi.org/10.6084/m9.figshare.11316281

Appendix A: Well water level response to aquifer pore pressure

The following differential equation describes water flow in and out of a well under semi-confined (leaky) conditions

$$\frac{\delta^2 s}{\delta r^2} + \frac{1\delta s}{r\delta r} - \frac{K's}{b'Kb} = \frac{S_s \delta s}{K\delta t}. \tag{A1}$$

Here, s is the drawdown in the aquifer, r is the radius from the centre of the well, K and S_s are the hydraulic conductivity and specific storage of the aquifer, b is the aquifer thickness (here assumed to be the length of the well screen), K' and b' are the hydraulic conductivity and thickness of the aquitard overlying the aquifer. Rojstaczer (1988) has solved this equation for harmonically varying flow in and out of the well with the following boundary conditions

$$s(\infty, t) = 0 \tag{A2}$$

and

$$\lim_{r \to 0} \frac{r\delta s}{\delta r} = \frac{\omega r_{ws}^2 \hat{x}}{2Kb} sin(\omega t). \tag{A3}$$

The solution for the drawdown just outside the well screen r_{ws} is

$$\hat{s}_w = \hat{x}_0 \cdot \hat{G}, \tag{A4}$$

and

$$\hat{G} = 0.5i \cdot W \cdot K_0 \left[\left[W^2 \left[S^2 + \frac{1}{q^2} \right] \right]^{0.25} \cdot \exp\left[0.5i \left[\mathrm{atan}(qS) \right] \right] \right] \cdot \exp(i\omega t). \tag{A5}$$

Here,

$$W = \frac{\omega r_{ws}^2}{Kb} \tag{A6}$$

and

$$q = \frac{\omega b'}{K'} \tag{A7}$$

and

$$\omega = 2\pi f. \tag{A8}$$

Further, K_0 is the modified Bessel function of the second kind of order zero.

The fluctuating water level and the drawdown are related by

$$\hat{x} = \hat{h}_f - \hat{s}_w, \tag{A9}$$

where $\hat{x}$ is the borehole water level, $\hat{h}$ is the subsurface pressure head and $\hat{s}$ is the drawdown. Equation A4 can be substituted into Equation A9 to form a complex ratio of the well water level response to changing pore pressure as

$$\hat{H} = \frac{1}{1+\hat{G}}. \tag{A10}$$

For fully confined conditions, when $K' \to 0$ and $b' \to \infty$ then the third term in Equation A1 becomes negligible and the analytical solution becomes the same as that solved by ~~Hsieh et al. (1988). In that case~~Hsieh et al. (1987). Hsieh et al. (1988) have shown that

$$\hat{h} = \frac{\hat{\epsilon}}{S_s} \tag{A11}$$

where ϵ is a strain. Using this relationship, the amplitude ratio and phase shift can be formulated as (Xue et al., 2016)

$$A_r = \text{abs}\begin{bmatrix} \hat{x} & \hat{x} \\ \hat{h} & \hat{\epsilon} \end{bmatrix} S_s = \frac{1}{\sqrt{(E^2+F^2)}} \tag{A12}$$

and

$$\Delta\phi = \arg\begin{bmatrix} \hat{x} & \hat{x} \\ \hat{h} & \hat{\epsilon} \end{bmatrix} = -tan^{-1}\left[\frac{F}{E}\right]. \tag{A13}$$

Here,

$$E = 1 - \frac{2\pi f r_{wc}^2}{2Kb}\left[\Psi Ker[\alpha_w] + \Phi Kei[\alpha_w]\right] \tag{A14}$$

and

$$F = \frac{2\pi f r_{wc}^2}{2Kb}\left[\Phi Ker[\alpha_w] - \Psi Kei[\alpha_w]\right], \tag{A15}$$

with

$$\Phi = -\frac{Ker_1[\alpha_w] + Kei_1[\alpha_w]}{\sqrt{2}\alpha_w(Ker_1^2[\alpha_w] + Kei_1^2[\alpha_w])} \tag{A16}$$

and

$$\Psi = -\frac{Ker_1[\alpha_w] - Kei_1[\alpha_w]}{\sqrt{2}\alpha_w(Ker_1^2[\alpha_w] + Kei_1^2[\alpha_w])} \tag{A17}$$

Here, Ker and Kei are the Kelvin functions of order zero, whereas Ker_1 and Kei_1 are the Kelvin functions of order one. Finally,

$$\alpha_w = \sqrt{\frac{\omega S_s b}{Kb}} r_{ws}. \tag{A18}$$

Appendix B: Calculating BE using the barometric response function

The well water level response to barometric pressure forcing in the time domain is referred to as the barometric response function (~~BRF~~BRF). A ~~BRF~~ BRF can be used to indicate confinement and estimate barometric efficiency (Rasmussen and Crawford, 1997; Spane, 2002). To account for time delays between changes in barometric pressure and their borehole water level changes, the differences are convoluted and the time coefficients are determined by least-squares regression. The method is as follows (Rasmussen and Crawford, 1997; Butler et al., 2011)

$$\min \sum_{n=0}^{N} \left[\Delta GW(t_n) - \sum_{k=0}^{K} [\alpha_k \Delta BP(t_n - \tau_k) + \beta_k \Delta ET(t_n - \tau_k)] \right]^2 \tag{B1}$$

where ΔGW, ΔBP and ΔET are the changes in borehole water level, barometric pressure, and Earth tides (potential, gravity or strains) respectively; t_n is the time of sample n; K is the total number of time lags with relative time $\tau_k = k\Delta t$; α_k and β_k are the time lag coefficients for the barometric and Earth tide response, respectively; Δt is the sampling period. It is a condition that $K \leq N$. The time-based barometric response function for is calculated as

$$BRF(\tau_k) = \sum_{k=0}^{K} \alpha_k(\tau_k). \tag{B2}$$

According to Rasmussen and Crawford (1997), the $BRF(t_k)$ has a characteristic shape that is indicative of the system's confinement. If a system is confined then BE can be calculated as (Rasmussen and Crawford, 1997)

$$BE = \max\left[BRF(\tau_k)\right]. \tag{B3}$$

This time-domain approach can also be used to remove barometric and Earth tide influences from the pressure head time series, for example to reveal small responses to pumping that are otherwise buried in the natural signals. We note that we do not further interpret the Earth tide lag coefficients β_k in this work.

Appendix C: Amplitude and phase uncertainty estimation

When HALS optimisation (Equation 12) is performed, a covariance matrix σ for the fitted coefficients a_c and b_c can be estimated. These can be propagated to obtain standard deviations for the amplitude (Equation 2) as

$$\sigma_{A_c} \approx \sqrt{\left(\frac{a_c}{A_c}\right)^2 \sigma_{a_c}^2 + \left(\frac{b_c}{A_c}\right)^2 \sigma_{b_c}^2 + \frac{2a_c b_c}{A_c^2}\sigma_{a_c b_c}}, \tag{C1}$$

and for the phase (Equation 3) as

$$\sigma_{\phi_c} \approx \sqrt{\left(\frac{b_c}{a_c^2+b_c^2}\right)^2 \sigma_{a_c}^2 + \left(\frac{-a_c}{a_c^2+b_c^2}\right)^2 \sigma_{b_c}^2 - \frac{2a_c b_c}{(a_c^2+b_c^2)^2}\sigma_{a_c b_c}}. \tag{C2}$$

This further allows propagation to aerial strain sensitivity as

$$\sigma_{A_c^{i,j}} \approx |A_c^{i,j}| \sqrt{\left(\frac{\sigma_{A_c^i}}{A_c^i}\right)^2 + \left(\frac{\sigma_{A_c^j}}{A_c^j}\right)^2}, \tag{C3}$$

and the phase shift as

$$\sigma_{\Delta\phi_c^{i,j}} \approx \sqrt{\sigma_{\phi_c^i}^2 + \sigma_{\phi_c^j}^2}. \tag{C4}$$

Here, the superscripts i and j stand for the two components that are related to each other, for example ET or GW.

Author contributions. GCR conceived the idea for this work, analysed the data, made the figures and wrote the first draft. MOC contributed to method development through intensive technical discussions and reviews. RIA and PB improved this work by providing useful suggestions and edits.

Competing interests. The authors declare that they have no conflict of interest.

Acknowledgements. This technical note is based on a presentation presented at the European Geosciences Union (EGU) general assembly in the year 2020 which was reorganised as Sharing Geosciences Online due to the COVID19 pandemic. We thank Paula Cutillo and Shannon Mazzei from the National Park Service (NPS) in California (USA) for providing the barometric and groundwater pressure dataset. This project has received funding from the European Union's Horizon 2020 research and innovation programme under the Marie Skłodowska-Curie grant agreement No 835852. MOC gratefully acknowledges funding for an Independent Research Fellowship from the UK Natural Environment Research Council (NE/P017819/1).

References

Acworth, R. I. and Brain, T.: Calculation of barometric efficiency in shallow piezometers using water levels, atmospheric and earth tide data, Hydrogeology Journal, 16, 1469–1481, https://doi.org/10.1007/s10040-008-0333-y, http://link.springer.com/10.1007/s10040-008-0333-y, 2008.

Acworth, R. I., Timms, W. A., Kelly, B. F., Mcgeeney, D. E., Ralph, T. J., Larkin, Z. T., and Rau, G. C.: Late Cenozoic paleovalley fill sequence from the Southern Liverpool Plains, New South Wales—implications for groundwater resource evaluation, Australian Journal of Earth Sciences, 62, 657–680, https://doi.org/10.1080/08120099.2015.1086815, 2015.

Acworth, R. I., Halloran, L. J. S., Rau, G. C., Cuthbert, M. O., and Bernardi, T. L.: An objective frequency domain method for quantifying confined aquifer compressible storage using Earth and atmospheric tides, Geophysical Research Letters, 43, 611–671, https://doi.org/10.1002/2016GL071328, http://dx.doi.org/10.1002/2016GL071328, 2016.

Acworth, R. I., Rau, G. C., Halloran, L. J. S., and Timms, W. A.: Vertical groundwater storage properties and changes in confinement determined using hydraulic head response to atmospheric tides, Water Resources Research, 53, 2983–2997, https://doi.org/10.1002/2016WR020311, http://dx.doi.org/10.1002/2016WR020311, 2017.

Agnew, D. C.: Baytap08: A Program for Analyzing Tidal Data, https://igppweb.ucsd.edu/~agnew/Baytap/baytap.html, 2008.

Agnew, D. C.: Earth Tides, Geodesy: Treatise on Geophysics, p. 163, 2010.

Allègre, V., Brodsky, E. E., Xue, L., Nale, S. M., Parker, B. L., and Cherry, J. A.: Using earth-tide induced water pressure changes to measure in situ permeability: A comparison with long-term pumping tests, Water Resources Research, 52, 3113–3126, https://doi.org/10.1002/2015WR017346, http://doi.wiley.com/10.1002/2015WR017346, 2016.

Bredehoeft, J. D.: Response of well-aquifer systems to Earth tides, Journal of Geophysical Research, 72, 3075–3087, https://doi.org/10.1029/JZ072i012p03075, http://doi.wiley.com/10.1029/JZ072i012p03075, 1967.

Butler, J. J., Jin, W., Mohammed, G. A., and Reboulet, E. C.: New insights from well responses to fluctuations in barometric pressure, Ground Water, 49, 525–533, https://doi.org/10.1111/j.1745-6584.2010.00768.x, http://doi.wiley.com/10.1111/j.1745-6584.2010.00768.x, 2011.

Clark, W. E.: Computing the barometric efficiency of a well, Journal of the Hydraulics Division, 93, 93–98, http://cedb.asce.org/CEDBsearch/record.jsp?dockey=0014622, 1967.

Cutillo, P. A. and Bredehoeft, J. D.: Estimating Aquifer Properties from the Water Level Response to Earth Tides, Ground Water, 49, 600–610, https://doi.org/10.1111/j.1745-6584.2010.00778.x, http://doi.wiley.com/10.1111/j.1745-6584.2010.00778.x, 2011.

Davis, D. R. and Rasmussen, T. C.: A comparison of linear regression with Clark's Method for estimating barometric efficiency of confined aquifers, Water Resources Research, 29, 1849–1854, https://doi.org/10.1029/93WR00560, http://doi.wiley.com/10.1029/93WR00560, 1993.

Gieske, A. and De Vries, J. J.: An analysis of earth-tide-induced groundwater flow in eastern Botswana, Journal of Hydrology, 82, 211–232, https://doi.org/10.1016/0022-1694(85)90018-6, https://linkinghub.elsevier.com/retrieve/pii/0022169485900186, 1985.

Hanson, J. M. and Owen, L. B.: Fracture Orientation Analysis by the Solid Earth Tidal Strain Method, https://doi.org/10.2118/11070-MS, https://doi.org/10.2118/11070-MS, 1982.

Hsieh, P. A., Bredehoeft, J. D., and Farr, J. M.: Determination of aquifer transmissivity from Earth tide analysis, Water Resources Research, 23, 1824–1832, https://doi.org/10.1029/WR023i010p01824, http://doi.wiley.com/10.1029/WR023i010p01824, 1987.

Hsieh, P. A., Bredehoeft, J. D., and Rojstaczer, S. A.: Response of well aquifer systems to Earth tides: Problem revisited, Water Resources Research, 24, 468–472, https://doi.org/10.1029/WR024i003p00468, http://dx.doi.org/10.1029/WR024i003p00468http://doi.wiley.com/10.1029/WR024i003p00468, 1988.

McMillan, T. C., Rau, G. C., Timms, W. A., and Andersen, M. S.: Utilizing the Impact of Earth and Atmospheric Tides on Groundwater Systems: A Review Reveals the Future Potential, Reviews of Geophysics, 57, 281–315, https://doi.org/10.1029/2018RG000630, https://onlinelibrary.wiley.com/doi/abs/10.1029/2018RG000630, 2019.

Merritt, M. L.: Estimating hydraulic properties of the Floridan Aquifer System by analysis of earth-tide, ocean-tide, and barometric effects, Collier and Hendry Counties, Florida, Tech. rep., https://doi.org/10.3133/wri034267, https://pubs.er.usgs.gov/publication/wri034267, 2004.

Rasmussen, T. C. and Crawford, L. A.: Identifying and Removing Barometric Pressure Effects in Confined and Unconfined Aquifers, Ground Water, 35, 502–511, https://doi.org/10.1111/j.1745-6584.1997.tb00111.x, http://doi.wiley.com/10.1111/j.1745-6584.1997.tb00111.x, 1997.

Rau, G. C.: PyGTide: A Python module and wrapper for ETERNA PREDICT to compute synthetic model tides on Earth, https://doi.org/10.5281/zenodo.1346260, https://doi.org/10.5281/zenodo.1346260, 2018.

Rau, G. C., Acworth, R. I., Halloran, L. J. S., Timms, W. A., and Cuthbert, M. O.: Quantifying Compressible Groundwater Storage by Combining Cross-Hole Seismic Surveys and Head Response to Atmospheric Tides, Journal of Geophysical Research: Earth Surface, 123, 1910–1930, https://doi.org/10.1029/2018JF004660, https://doi.org/10.1029/2018JF004660http://doi.wiley.com/10.1029/2018JF004660, 2018.

Ritzi, R. W., Sorooshian, S., and Hsieh, P. A.: The estimation of fluid flow properties from the response of water levels in wells to the combined atmospheric and Earth tide forces, Water Resources Research, 27, 883–893, https://doi.org/10.1029/91WR00070, http://doi.wiley.com/10.1029/91WR00070, 1991.

Roeloffs, E. A., Burford, S. S., Riley, F. S., and Records, A. W.: Hydrologic effects on water level changes associated with episodic fault creep near Parkfield, California, Journal of Geophysical Research, 94, 12 387, https://doi.org/10.1029/jb094ib09p12387, http://doi.wiley.com/10.1029/JB094iB09p12387, 1989.

Rojstaczer, S.: Determination of fluid flow properties from the response of water levels in wells to atmospheric loading, Water Resources Research, 24, 1927–1938, https://doi.org/10.1029/WR024i011p01927, 1988.

Rojstaczer, S. and Agnew, D. C.: The influence of formation material properties on the response of water levels in wells to Earth tides and atmospheric loading, Journal of Geophysical Research, 94, 12 403, https://doi.org/10.1029/JB094iB09p12403, http://doi.wiley.com/10.1029/JB094iB09p12403, 1989.

Spane, F. A.: Considering barometric pressure in groundwater flow investigations, Water Resources Research, 38, 14–1, https://doi.org/10.1029/2001WR000701, http://www.agu.org/pubs/crossref/2002/2001WR000701.shtml, 2002.

Tary, J. B., Herrera, R. H., Han, J., and Van Der Baan, M.: Spectral estimation - What is new? What is next?, Reviews of Geophysics, 52, 723–749, https://doi.org/10.1002/2014RG000461, http://doi.wiley.com/10.1002/2014RG000461, 2014.

Toll, N. J. and Rasmussen, T. C.: Removal of Barometric Pressure Effects and Earth Tides from Observed Water Levels, Ground Water, 45, 101–105, https://doi.org/10.1111/j.1745-6584.2006.00254.x, https://www.semanticscholar.org/paper/Removal-of-barometric-pressure-effects-and-earth-Toll-Rasmussen/4df94fbcccb1257787802056ab4554a6bb0809dchttp://doi.wiley.com/10.1111/j.1745-6584.2006.00254.x, 2007.

Turnadge, C., Crosbie, R. S., Barron, O., and Rau, G. C.: Comparing Methods of Barometric Efficiency Characterization for Specific Storage Estimation, Groundwater, 57, 844–859, https://doi.org/10.1111/gwat.12923, https://onlinelibrary.wiley.com/doi/abs/10.1111/gwat.12923, 2019.

Van Camp, M. and Vauterin, P.: Tsoft: graphical and interactive software for the analysis of time series and Earth tides, Computers & Geosciences, 31, 631–640, https://doi.org/10.1016/j.cageo.2004.11.015, http://linkinghub.elsevier.com/retrieve/pii/S0098300404002456, 2005.

van der Kamp, G. and Gale, J. E.: Theory of earth tide and barometric effects in porous formations with compressible grains, Water Resources Research, 19, 538–544, https://doi.org/10.1029/WR019i002p00538, http://dx.doi.org/10.1029/WR019i002p00538, 1983.

Wenzel, H.-G.: The nanogal software: Earth tide data processing package ETERNA 3.30, Bulletin d'Informations Mareés Terrestres, 124, 1996.

Xue, L., Brodsky, E. E., Erskine, J., Fulton, P. M., and Carter, R.: A permeability and compliance contrast measured hydrogeologically on the San Andreas Fault, Geochemistry, Geophysics, Geosystems, 17, 858–871, https://doi.org/10.1002/2015GC006167, https://doi.org/10.1002/2015GC006167, 2016.